The Numerical Simulation of Jet Mixing With Steady and Antisymmetric Pulsed Jets in Different Frequency

R B Zhang[1], L Hong[1]

[1] School of Energy and Power Engineering, Beihang University, XueYuan Road No.37, HaiDian District, Beijing 100191, China

493719943@qq.com

Abstract. A parametric study of the effect of rectangular antisymmetric pulsed control jets on the jet mixing with different pulse frequency is conducted using RANS simulation. The mean centerline potential core length and the axial velocity contours of the main jet at different downstream positions (*x/D*) is investigated and discussed in detail. When the antisymmetric pulsed control jets are injected into the main flow, a starting vortex is observed in the axial velocity contours on x-z plane, which does not exist when the control jets are symmetric steady (*St*=0). The factors that have effect on the jet mixing are analyzed and described in detail, and the jet/ambient air interfacial area is found to play an important role in jet mixing. The best mixing effect can be reached at the same mass flow ratio of the main flow to the control jets if a proper pulse frequency of the control jets is used.

1. Introduction

The jet mixing enhancement is significantly useful for jet engines to reduce the jet potential core length [1,2] and the infrared emissions [3]. There are many ways to achieve it which could be characterized as the active control technology [4-7] and the passive control technology [8,9]. The active flow control technology [10] is introducing energy or auxiliary power into the flow [11,12]. The working parameters can be adjusted according to the state of the engine to achieve the desired mixing effect and the CJs can be switched off when not needed, which results in the reduction of the drag or thrust loss penalty [13] compared to the passive technology. Therefore, extensive investigations have been carried out in this area in the last few decades.

In 1994, R Howard [14] et al. studied the mixing effect when a pulsed control jet injected into a supersonic crossflow and found that the flow penetration is deeper than steady injection. D E Parekh [15] et al. used novel piezoelectric excitation devices for high frequency and high intensity injections into subsonic and supersonic shear layers and found that the mixing effect has a significant increased because of the flapping mode, and the optimum excitation Strouhal number is around 0.2 when the

injection flow rates was as little as 1%. B F Jonathan [16] et al. found that the jet's development can be significantly altered when high-amplitude, low mass flux pulsed jets blowing normal to a jet's shear layer near the nozzle, and it appears to overwhelm the turbulence, resulting in nearly the same effect no matter how high and low the Reynolds numbers are. Besides, the jet mixing forcing at Sr = 0.2 is more effective, which is consistent with previous research conclusions. The research mentioned above are all studied using experiment, and B Parviz [17] et al. studied both experimentally and computationally. It is found that fluid tabs produce the same streamwise vortex formation process as solid tabs, which is confirmed in [18]. J K Sutariya [19] et al. experimentally investigated the supersonic mixing effect under different frequencies and pulse widths, and the results were compared with the results of continuous injection. Better mixing is found using pulsed injection and mixing is enhanced as pulse width decreases. In addition to the parametric research of the jet mixing effect which is conducted experimentally [20] and numerically (such as URANS [21] and Large Eddy [22]), the mechanics and the starting vortex are also studied [23-25].

The starting vortex discussed above is only studied in single pulsed jet. But in this paper, a starting vortex is observed when two antisymmetric pulsed control jets injected verticality into the main flow. And the current study parametrically investigates the jet mixing effect with different pulse frequencies using numerical simulations, providing a better understanding of the mechanisms that the influence on the jet mixing enhancement by using velocity contours and streamlines on different planes. In addition, the parameters affecting the mixing effect are summarized, and the optimum pulse frequency are found which can be used to achieve the best mixing effect at the same mass flow rate.

2. Computation scheme

2.1. Simulation methods

All the numerical simulations in the present work are conducted using ANSYS FLUENT software. And the Reynolds-Averaged Navier-Stokes (RANS) Renormalization Group (RNG) k-ε turbulence model is used in the current study.

2.2. Geometric model, Mesh generation and Boundary conditions

2.2.1. Geometric model. The cross-section of a 3D axisymmetric nozzle with CJs [26] is shown in figure 1. The flow direction of the main jet and CJs is indicated along X and Z direction respectively. The nozzle inlet diameter D_{in} is 203.2mm and the nozzle outlet diameter D_{out} equals to 101.6mm, a short parallel extension with the length of 127mm was connected to the nozzle outlet to smooth the main flow. The two actuators in green are distributed in the top and bottom of the nozzle outlet and attached to it. The value of width b of CJs is 43.18mm.

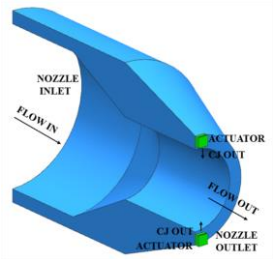

Figure 1. Schematic of 3D axisymmetric nozzle with CJs.

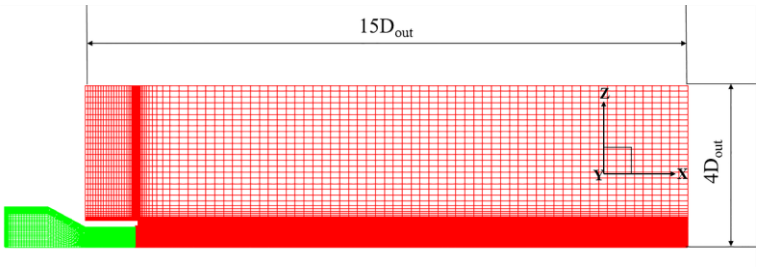

Figure 2. Cross-section of the solution domain and mesh structure: *x*-*z* plane.

2.2.2. Solution domain and mesh generation. The solution domain is shown in figure 2. It includes the nozzle and the entire jet flow area. In order to save the computation time, the simulation is conducted in a quarter of the entire domain since the nozzle is axisymmetric and the two actuators are symmetrically distributed on X-axis. In order to accurately simulate the interaction between the main jet and the CJ, the grids near the actuators are refined.

2.2.3. Boundary conditions. Incompressible ideal gas is used in the simulation because of the low flow velocity. The flow velocity at the nozzle inlet is 2.5m/s with the static temperature of 296.03K. The CJs are antisymmetrically injected into the main jet. Multiple CJ's pulse frequencies are used as shown in table 1 and the dimensionless pulse frequency of CJs *St* will be applied in the following passage. The pressure of the ambient air is 1 atm. The wall boundary condition is applied in the inner walls and the outer walls of the nozzle as well as the CJs.

Table 1. The geometry parameters and pulse frequencies of CJs.

a/mm	*b*/mm	*v*/m/s	*f*/Hz	*St* (f*D_{out}/U_j)
2.032	43.18	9.57	0	0
		19.15	5	0.05
			15	0.14
			20	0.19
			30	0.29
			40	0.38

3. Results and discussion

Numerical simulations of the jet mixing effect using the geometric model [26] have been performed for different pulse frequencies of antisymmetric CJs *St* at the same mass flow rate which equals to 1%. The predicted result with clean jet is also performed as the baseline to assess the jet mixing effect. The results and analysis of each case are described in detail in the following paragraphs.

3.1. Comparison between symmetric steady jets (St=0) and antisymmetric pulsed jets (St=0.14)

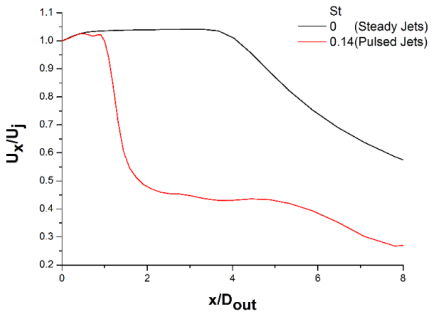

Figure 3. Normalized axial velocity of the primary jet centerline under steady jets (*St*=0) and pulsed jets (*St*=0.14).

The axial velocity distribution of the main jet centerline with nondimentional pulse frequency *St* of 0 and 0.14 are shown in figure 3 to characterize the jet mixing behavior. When *St* is 0, the CJs are essentially symmetric steady jets, which means that the excitation method is different from the pulsed jets. Besides, when St is 0.14, the axial velocity distribution of the main jet centerline is time-averaged. When *St* is 0, the centerline potential core length is $3.68D_{out}$, and when *St* increases to 0.14, the centerline potential core length decreases to $0.93D_{out}$. This indicates that the pulsed CJs have more pronounced effect on enhancing the jet/ambient mixing than the steady jets (*St*=0).

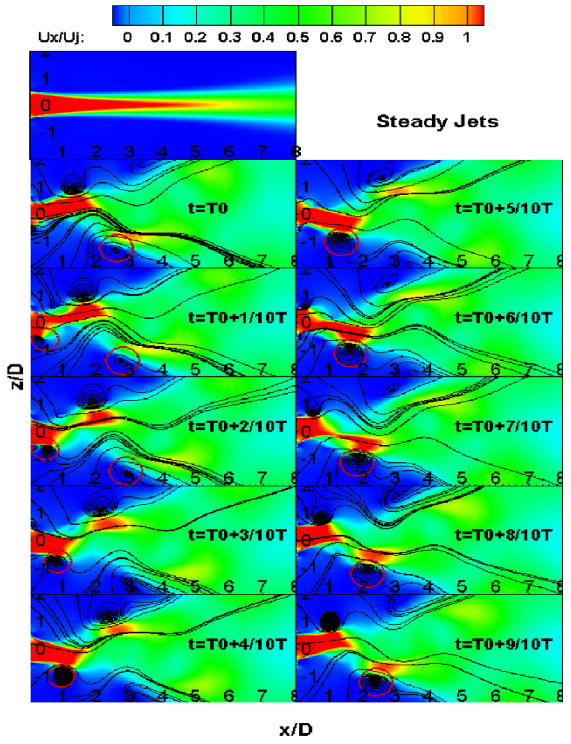

Figure 4. The axial velocity contour on x-z plane under steady jets (*St*=0) and pulsed jets (*St*=0.14) at different time instants.

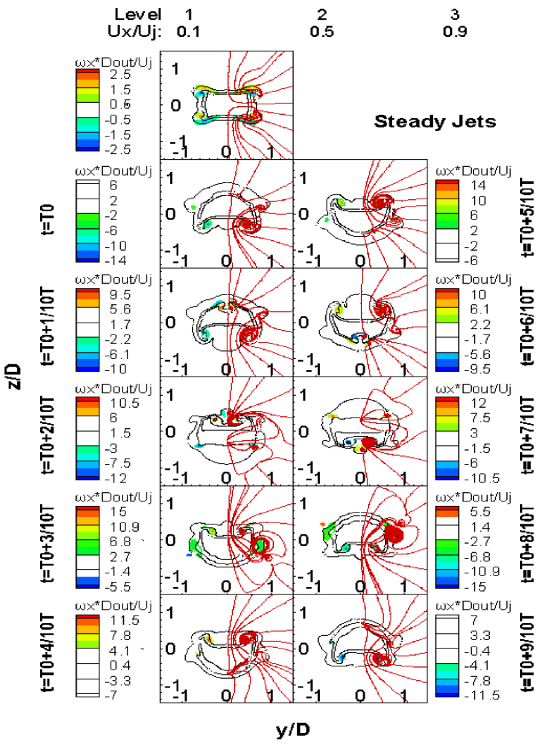

Figure 5. The axial velocity contour on y-z plane at x=Dout under steady jets (*St*=0) and pulsed jets (*St*=0.14) at different time instants.

In order to further analyze the effect of using symmetric steady jets (*St*=0) and antisymmetric

pulsed jets on jet mixing, the contours of axial velocity on x-z plane are shown in figure 4. When the *St* is 0, there is a potential core contraction on x-z plane, but there is a flapping mode in the potential core area on x-z plane when the excitation method changes to antisymmetric pulsed jets. And the flapping frequency is consistent with the pulse frequency. Differ from symmetric steady jets (*St*=0), the expansion of the low-speed boundary of shear layer is more obvious along with a very large expansion area on x-z plane.

A vortex can be seen on x-z plane when the *St* is 0.14, which does not exist in symmetric steady jets (*St*=0). With the increase of time instant, the vortex is getting larger and moving to downstream on x-z plane. When the main jet is excited by the antisymmetric pulsed jets, downstream of the main jet breaks off with upstream of the main jet, which is equivalent to generating a new jet at downstream. The formation process of the vortex observed in figure 4 are similar to the vortex ring of starting jets [28], so it is called starting vortex. The ambient air will be entrained into the primary jet through the starting vortex, further improving the jet/ambient air mixing and further changing the shape of the primary jet.

The axial velocity contour lines, streamlines and the streamwise vorticity of symmetric steady jets (*St*=0) and antisymmetric pulsed jets at different time instants on y-z plane at $x=D_{out}$ are shown in figure 5. There are only two pair of counter rotating vortices when *St* is 0, but there are at least two pair of counter rotating vortices when the CJs changes to antisymmetric pulsed jets, the number of the streamwise vorticities is even up to four at some time instants. Although the streamwise vorticities of symmetric steady jets (*St*=0) reside on the low-speed boundary of the shear layer, the size and the intensity are smaller than the streamwise vorticities of antisymmetric pulsed jets. Besides, when *St* is 0.14, the shape of the primary jet deforms more significantly than using the steady jets (*St*=0) as CJs.

3.2. Comparison between antisymmetric control jets with different pulse frequency

The mixing metric *U** was defined as the average velocity for the antisymmetric pulsed control jets measured at $10D_{out}$ divided by the average velocity for the clean jets at $10D_{out}$. It can be seen in figure 6 that the optimum pulse frequency *St* is 0.14 in the present study and the mixing metric *U** decreases to 0.39. This indicates that the antisymmetric pulsed jets have a great effect on enhancing the jet/ambient mixing when they are injected into the main jet with *St* of 0.14.

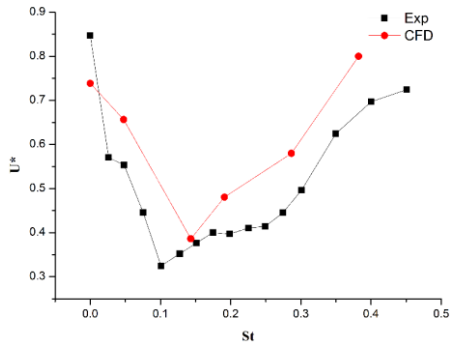

Figure 6. The mixing metric *U** with different *St*.

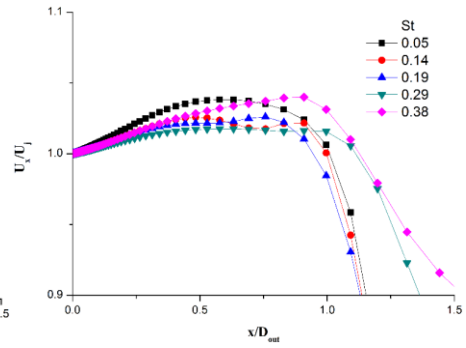

Figure 7. Normalized centerline axial velocity under different *St*.

As is shown in figure 7, the centerline potential core lengths with different pulse frequency *St* are all around D_{out}. The shortest centerline potential core length can be seen when *St* is 0.19, which is different from the mixing metric *U**'s optimum pulse frequency *St*.

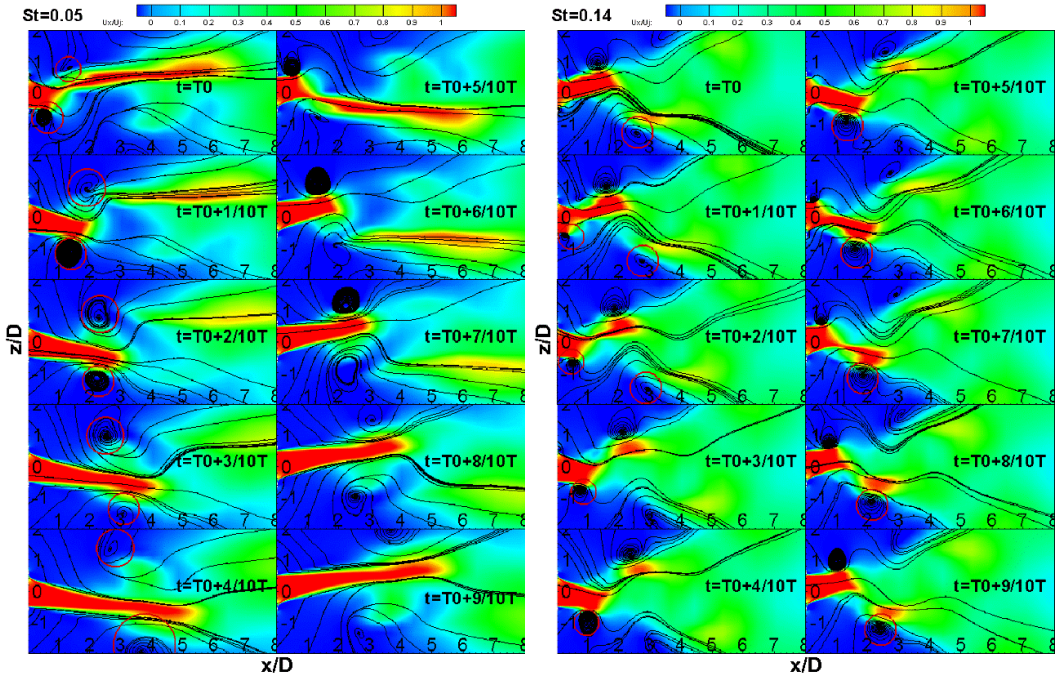

(a)

(b)

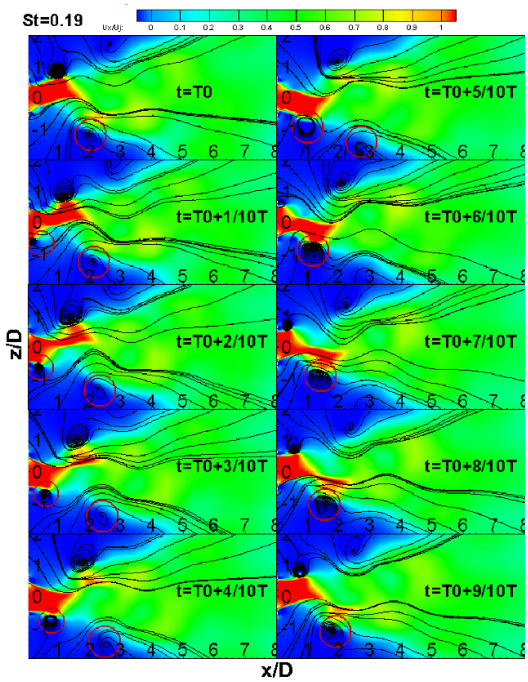

(c)

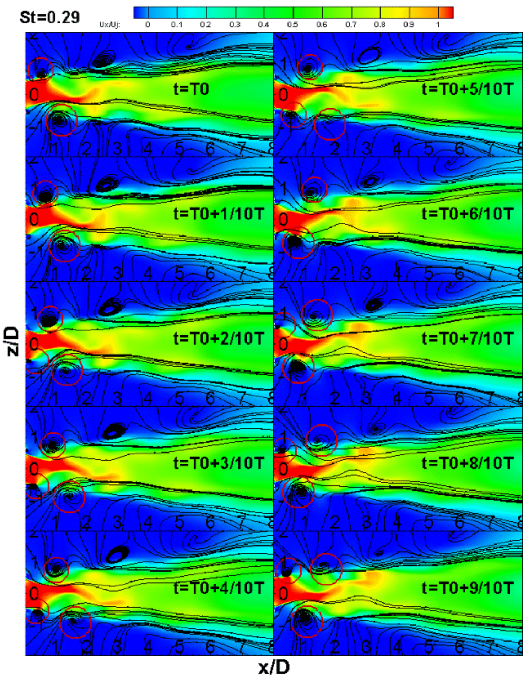

(d)

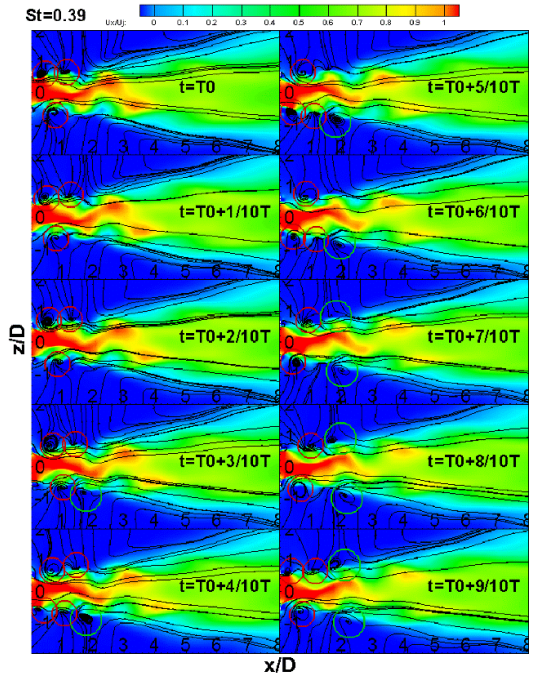

(e)

Figure 8. The axial velocity contour on x-z plane under different pulse frequency (*St*) at different time instants.

Figure 8 shows the axial velocity contour and streamlines on x-z plane under different pulse frequency (*St*) at different time instants. When antisymmetric pulsed jets are injected and the flapping frequency of the upstream potential core is consistent with *St*, under all the pulse frequencies. However, for downstream potential core which breaks off with the upstream because of the antisymmetric pulsed jets, the flapping frequency is consistent with the pulse frequency when *St* is 0.05, 0.14 and 0.19, and when St increases to 0.29 and 0.39, the flapping frequency is not consistent with the pulse frequency any longer. Besides, the flapping amplitude is obvious when *St* is 0.05, 0.14 and 0.19, and when *St* increases to 0.29 and 0.39, the flapping amplitude is very tiny.

When *St* is 0.05, the shape of the potential core changes a lot as the time instant increases, and the potential core length increases a lot, at the time instant of T0+4/10T, it even increases to more than $5D_{out}$. In addition, the potential core length of this case is the longest when compared with the other four pulse frequency cases at the same time instant. When *St* increases, both of the shape and the length of the potential core change a little as the time instant increases. The potential core length decreases at first, but then it begins to increase when *St* increased to 0.29.

In figure 8, an expansion can be observed in all the five cases on x-z plane. When *St* is 0.05, the expansion area is large which indicates that it is effective to spread the jet to downstream. As *St* increases to 0.14 and 0.19, the expansion area is getting larger, this means that spreading the jet to downstream is more effective. But when *St* continues to increase to 0.29, the expansion area decreases. When *St* increases to 0.39, the largest pulse frequency studied here, the expansion area increases compared with the expansion area when *St* is 0.29, but still smaller than the cases whose *St* is 0.05, 0.14 and 0.19, respectively. It is supposed that the expansion area is related to the flapping amplitude.

Starting vortex is observed in figure 8 using streamlines in all the five cases, but the details of the starting vortex are different. When *St* is 0.05, there are two starting vortex on both sides of the main jet,

and both of the two starting vortex forms at the first time instant and close to the nozzle, however the starting vortex opposite to the working pulsed jet is closer to the nozzle than the other starting vortex, then the two starting vortex are getting bigger and moves to downstream as time increases, and at the fifth time instant, the starting vortex opposite to the working pulsed jets stops at x=4D_{out} and the other starting vortex stops at x=3D_{out}. When the other pulsed jet starts to work at the sixth time instant, both of the two starting vortex disappear and the phenomenon above appears once every half cycle. When *St* increases to 0.14 and 0.19, there is only one starting vortex forms at the second time instant, opposite to the working pulsed jet and the formation position is very close to the nozzle. Both of the two starting vortex stops at x=3D_{out} and the existence time is 1.2 cycles and 1.5 cycles, respectively. And when the other pulsed jet starts to work after half cycle, there will be the same developing process of the starting vortex, which is the same as the case when *St* is 0.05. When *St* increases to 0.29, the developing process of the starting vortex is more complicated. Because of the flapping frequency of the downstream is not consistent with the pulse frequency, and the starting vortex far from the nozzle has little effect on the jet mixing, so only the starting vortex marked with the red circle is concerned. The same as *St* of 0.14 and 0.19, there is only one starting vortex, but it forms at the third time instant, opposite to the working pulsed jet and the formation position is very close to the nozzle. Its stop position and existence time are not sure but the same developing process of the starting vortex once every half cycle. As for *St* of 0.39, the starting vortex is too complicated to find a developing law. The main starting vortex marked with red cycle forms at the fifth time instant, and its form frequency is consistent with the pulse frequency. In addition, it is worth to note that there is another starting vortex marked with green cycle, far from the nozzle, and it is supposed to be introduced when the main jet is spreading to downstream.

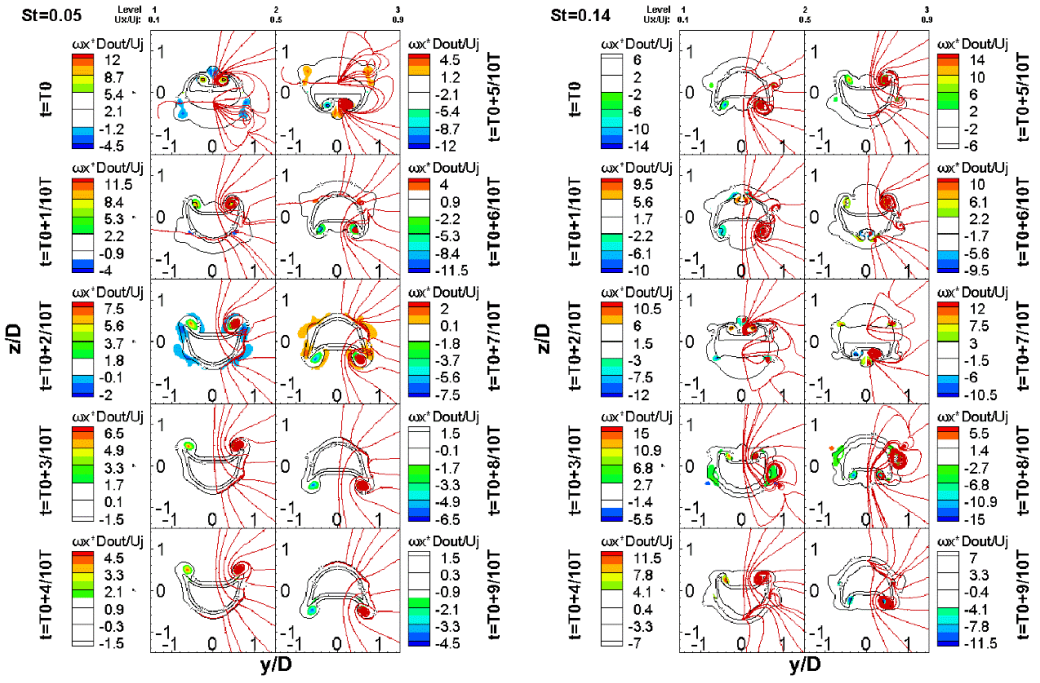

(a) (b)

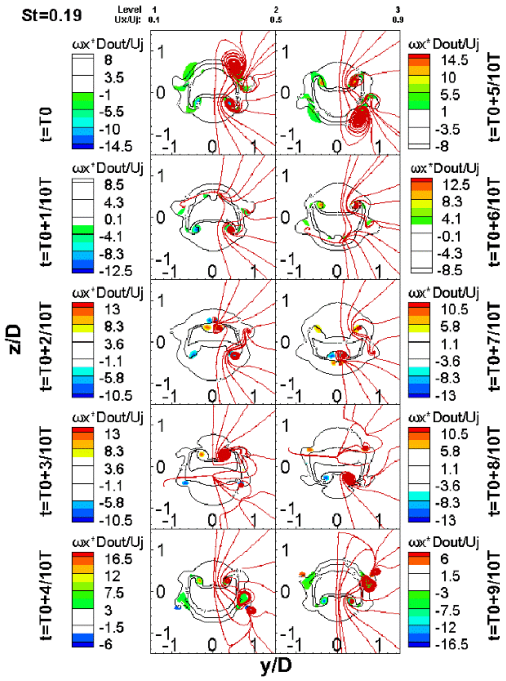

(c)

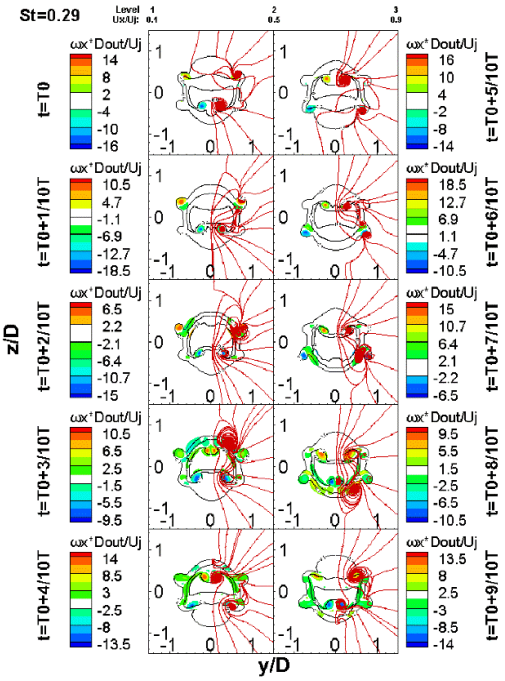

(d)

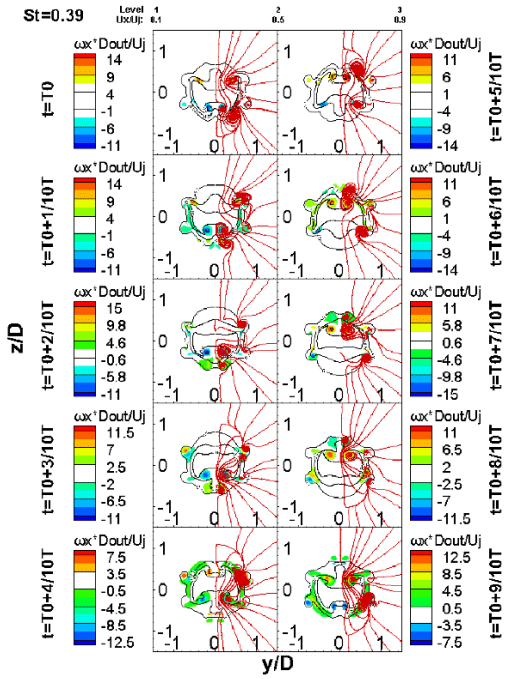

(e)

Figure 9. The axial velocity contour on y-z plane at $x=D_{out}$ under different pulse frequency (*St*) at different time instants.

Figure 9 shows the axial velocity contour on y-z plane at $x=D_{out}$ under different pulse frequency (*St*) at different time instants. It is found that all the main jet section shape of the five cases deformed dramatically when antisymmetric pulsed jets injected into the main jet. There is only one pair streamwise vortex in figure 9a, it resides on the low-speed side of the shear layer which can help to

entrain large ambient air and result in a great mixing effect. There are at least two pair streamwise vortex when *St* is 0.14, 0.19, 0.29 and 0.39. However, only the vortex which is on the low-speed side of the shear layer can make more ambient air entrained which leads to a better mixing effect, so only the number and the size of these vortex have a great effect on jet mixing. When *St* is 0.14 and 0.19, the number and the size of the vortices which are close to the low-speed boundary of the shear layer is larger than other cases. This is an important reason that explains why the cases pulsed with *St* of 0.14 and 0.19 can have a better mixing effect when assessed with the mixing metric *U** and centerline potential core length.

4. Conclusions

A parametric study of the effects of antisymmetric pulsed CJs on the jet mixing of using different pulse frequency (*St*) have been conducted and the conclusions are listed as follows:

(1) When the main jet is excited with symmetric steady jets (*St*=0) at a mass flow rate of 1%, the mixing metric *U** is 0.74 and its centerline potential core length is $3.68D_{out}$, but when the excitation method changes to antisymmetric pulsed jets (*St*=0.14), the mixing metric *U** decreases to 0.39 and its centerline potential core length decreases to $0.93D_{out}$. Besides, a starting vortex is observed when antisymmetric pulsed jets (*St*=0.14) are injected into the main jet, and it does not exist when using the symmetric steady jets (*St*=0). So a better mixing effect is observed when using antisymmetric pulsed jets, no matter which evaluation method of mixing effect is used.

(2) When the whole jet/ambient mixing effect is concerned, then the minimum mixing metric *U** is 0.39 and the optimum pulse frequency *St* correspond to it is 0.14. When only infrared radiation of the main jet is concerned, the minimum centerline potential core length which reflects the mixing effect near the nozzle is observed when *St* is 0.19, which means that 0.19 is the optimum pulse frequency *St*.

(3) It is found that the jet/ambient interfacial area is an important factor to effect the jet mixing. And there are three factors that affect the jet/ambient interfacial area: 1) a flapping mode is generated by using antisymmetric pulsed jets, which results in a significant deformation of the main jet, and thus the jet/ambient interfacial area increases dramatically; 2) a starting vortex is found when the CJs are antisymmetric pulsed jets, and the longer it exists, the more ambient air will be entrained, as a result, the deformation of the primary jet is intensified, leading to a further increase in the jet/ambient air interfacial area; 3) the number and the size of the streamwise vorticities which are on the low-speed side of the shear layer are also important to the jet/ambient air interfacial area. The three poins above can explain why 0.14 and 0.19 are the optimum pulse frequency *St* when assessed with the mixing metric *U** and centerline potential core length, respectively.

5. References

[1] Valdis K, John D, David M S and Michael F M 1999 *30th AIAA Fluid Dynamics Conf.* 1999 Jun 28-Jul 1 Norfolk VA USA American Institute of Aeronautics and Astronautics 3507 pp 1-12

[2] Robert F, Ahuja K K, Brian C and Cacye B 2004 *10th AIAA/CEAS Aeroacoustics Conf.* 2004 May 10-12 Manchester England UK American Institute of Aeronautics and Astronautics 2874 pp 1-9

[3] Clarence F C, John D, David S and Valdis K 2000 *AIAA Fluid 2000 Conf .and Exhibit* 2000 Jun 19-22 Denver CO USA American Institute of Aeronautics and Astronautics 2471 pp 1-11

[4] Sun LY, Terrence W S, Susan C M, Mounir I, David G and Roy T 2008 *6th Int. Energy*

Conversion Engineering Conf. (IECEC) 2008 Jul 28-30 Cleveland Ohio USA American Institute of Aeronautics and Astronautics 5719 pp 1-17

[5] Samimy M, Kim J H, Kastner J, Adamovich I and Utkin Y 2007 Active control of a mach 0.9 jet for noise mitigation using plasma actuators *AIAA Journal* **45** 890-901

[6] Adnan E and Robert E B 2001 Structure, penetration, and mixing of pulsed jets in cross flow *AIAA Journal* **39** 417-23

[7] Ritchie B D, Mujumdar D R and Seitzman J M 2000 *38th Aerospace Sciences Meeting & Exhibit* 2000 Jan 10-13 Reno NV USA American Institute of Aeronautics and Astronautics 0404 pp 1-8

[8] Tong F and James J M 2006 *3rd AIAA Flow Control Conf.* 2006 Jun 5-8 San Francisco California USA American Institute of Aeronautics and Astronautics 3702 pp 1-12

[9] Callender B and Gutmark E 2003 *9th AIAA/CEAS Aeroacoustics Conf. and Exhibit* 2003 May 12-14 Hilton Head South Carolina USA American Institute of Aeronautics and Astronautics 3210 pp 1-16

[10] Linda D K Active flow control technology. *ASME Fluids Engineering Division Technical Brief* pp 1-28

[11] Jonathan B F and Parviz M 1998 *1998 ASME Fluids Engineering Division Summer Meeting* 1998 Jun 21-25 Washington DC USA The American Society of Mechanical Engineers 5235 pp 1-6

[12] Johari H, Pacheco T M and Hermanson J C 1998 Penetration and mixing of fully-pulsed turbulent jets in crossflow *AIAA Journal* http://arc.aiaa.org DOI: 10.2514/6.1998-2908

[13] Muhammad A K and James J M 2015 Unsteady predictions of mixing enhancement with steady and pulsed control jets *AIAA Journal* **53** 1262-76

[14] Howard R and Larry C 1994 Pulsed jets in supersonic crossflow *J. PROPULSION* **10** 746-8

[15] Parekh D E, Kibens V, Glezer A, Wiltse J M and Smith D M 1996 *AIAA 34th Aerospace Sciences Meeting and Exhibit* 1996 Jan 15-18 Reno NV USA American Institute of Aeronautics and Astronautics 0308 pp 1-24

[16] Jonathan B F and Parviz M 2000 Jet mixing enhancement by high-amplitude fluidic actuation *AIAA Journal* **38** 1863-70

[17] Parviz B and James J M 2004 *2nd AIAA Flow Control Conf.* 2004 Jun 28- Jul 1 Portland Oregon USA American Institute of Aeronautics and Astronautics 2401 pp 1-13

[18] Parviz B, Tong F and James J M 2008 Active flow control of jet mixing using steady and pulsed fluid tabs *IMechE* **222** 381-92

[19] Sutariya J K and Job K 2007 *43rd AIAA/ASME/SAE/ASEE Joint Propulsion Conf. & Exhibit* 2007 Jul 8-11 Cincinnati OH USA American Institute of Aeronautics and Astronautics 5032 pp 1-12

[20] Toshinori K, Noboru S, Muneo I and Sadatake T 2007 *43rd AIAA/ASME/SAE/ASEE Joint Propulsion Conf.& Exhibit* 2007 Jul 8-11 Cincinnati OH USA American Institute of Aeronautics and Astronautics 5405 pp 1-12

[21] Kouchi T, Sasaya K, Watanabe J, Sibayama H and Masuya G 2010 *46th AIAA/ASME/SAE/ASEE Joint Propulsion Conf. & Exhibit* 2010 Jul 25-28 Nashville TN USA American Institute of Aeronautics and Astronautics 6645 pp 1-10

[22] Ramya P, Joseph S, Jerry S, Jeff J and Suresh M 2010 *48th AIAA Aerospace Sciences Meeting Including the New Horizons Forum and Aerospace Exposition* 2010 Jan 4-7 Orlando Florida

USA American Institute of Aeronautics and Astronautics 1288 pp 1-12
[23] Geng T, Zheng F, Kuznetsov A V and Roberts W L 2007 *43rd AIAA/ASME/SAE/ASEE Joint Propulsion Conf. & Exhibit* 2007 Jul 8-11 Cincinnati OH USA American Institute of Aeronautics and Astronautics 5051 pp 1-17
[24] Yu S C M, Ai J J, Gao L and Law A W K 2008 Vortex formation process of a starting square jet *AIAA Journal* **46** 223-31
[25] Gao L and Yu S C M 2016 Formation of leading vortex pair in two-dimensional starting jets *AIAA Journal* **54** 1364-9
[26] Paul W 2007 Jet mixing enhancement by high amplitude pulse fluidic actuation [dissertation] Ann Arbor (48106-1346) Georgia Institute of Technology
[27] Muhammad A K and James J M 2011 Subsonic jet mixing via active control using steady and pulsed control jets *AIAA Journal* **49** 712-24
[28] Geno P, Carolina M C, Carlos M B and Pedro G H 2007 Experimental characterization of starting jet dynamics *Fluid Dynamics Research* **39** 711-30

Acknowledgments
The author gratefully acknowledge the support from the National Nature Science Foundation of China (Grants: 11572027).